The Bering Sea Regional Data Assimilation System: From Climate Variability to Short Term Hindcasting

Gleb G. Panteleev, Max Yaremchuk, Vladimir Luchin and Oceana Francis

Introduction

In the last decades, 4d variational (4dVar) data assimilation (DA) has become the most acknowledged tool for advanced hindcasting and forecasting of the ocean circulation. Starting from DA systems constrained by simple dynamics (e.g., [1, 16]), the 4dVar approach [9] has gradually evolved into advanced DA systems based on state-of-the-art ocean models (MIT, ROMS) and is now routinely applied toward reconstructing the circulation in the Arctic, Pacific, or World Ocean (e.g., [5, 15]). These state-of-the-art DA systems involve the assimilation of a variety of observations from satellites, surface and Argo drifters and climatological observations from oceanographic databases. Assimilation of these publicly accessible, near real-time observations is natural since the major goal of the "global" DA systems is to provide hindcasting of the global circulation and/or analysis of observed climate changes on a global scale.

Meanwhile, due to the low flexibility of the global DA systems in assimilating regional data on smaller scales, the regional DA systems have been under extensive development within the last decade (e.g. [6, 8]). These DA systems routinely assimilate alongtrack satellite altimetry (Jason-1, Jason-2, CryoSat), hourly SSTs from GOES, and surface currents from HFRs and provide regional updates and 3-day forecasts of the ocean state. It is necessary to note, that all the regional

G. G. Panteleev (✉) · M. Yaremchuk
Naval Research Laboratory, Stennis Space Center, Hancock, USA
e-mail: gleb.panteleev@nrlssc.navy.mil

V. Luchin
Pacific Oceanological Institute, Vladivostok, Russia
e-mail: vlad_luchin@mail.ru

O. Francis
University of Hawaii, Honolulu, USA
e-mail: oceanaf@hawaii.edu

M. G. Velarde et al. (eds.), *The Ocean in Motion*, Springer Oceanography,
https://doi.org/10.1007/978-3-319-71934-4_32

systems were developed in the domains where TS observations were routinely collected year-round for a long period of time. This allows for reliable estimation of the background state, which is one of the key components of any DA system (e.g. [32]). There are, however, many regions where the temporal and spatial distribution of the observations is irregular and/or sparse in time and space. A prominent example is the Bering/Chukchi Sea basin which becomes increasingly important due to the rapid growth of the sea traffic and emerging prospects for development of oil and mining industries on the shelves.

In this contribution, we discuss the key components of the regional Bering Sea DA system developed by the authors in recent years [21, 22, 25] and present results of the analysis of the Bering Sea circulation on different scales.

The Regional 4dVar Data Assimilation System

The dynamic components, which synthesize diverse oceanographic data within a single framework are the Semi-Implicit Ocean Model (SIOM) and its adjoint configured to optimize the SIOM trajectory with respect to observations. The SIOM is a modification of the C-grid, z-coordinate Ocean Global Circulation Model (OGCM) developed at the Laboratoire d'Oceanographie Dynamique et de Climatologie [12]. The model was specifically designed for operating within the regional 4dVar framework controlled by fluxes at the open model boundaries and sea surface. The model is semi-implicit both in barotropic and baroclinic modes, permitting simulations with relatively large time steps of approximately 0.1 day [17, 20–22]. The tangent linear model was obtained by direct differentiation of the forward model code. The adjoint code of the model was built analytically by transposition of the operator of the tangent linear model, linearized in the vicinity of the given solution of the forward model [32]. The spatial structure of the background error covariances is modeled by the quadratic polynomials of the Laplacian operator [34, 35].

The SIOM 4dVar DA system supports assimilation of diverse oceanographic data such as: (a) In situ, *Temperature and salinity* observations from the database of the Far Eastern Branch of the Russian Academy of Science; (b) *Historical velocity observations* from moorings and sea surface drifters, and satellite-tracked drifter trajectories (Fig. 1b); (c) *Estimates of the mean transport through the Bering Strait.* Mean climatological estimates of 0.9 ± 0.2 Sv and corresponding seasonal transport are taken from [31]; (d) *Atmospheric forcing data* (momentum, heat and salt fluxes) for assimilation are taken from the National Center for Environmental Prediction (NCEP); (e) *The SSH anomalies* from the AVISO database at http://www.aviso.altimetry.fr. All observations are supplied with corresponding spatially varying covariances.

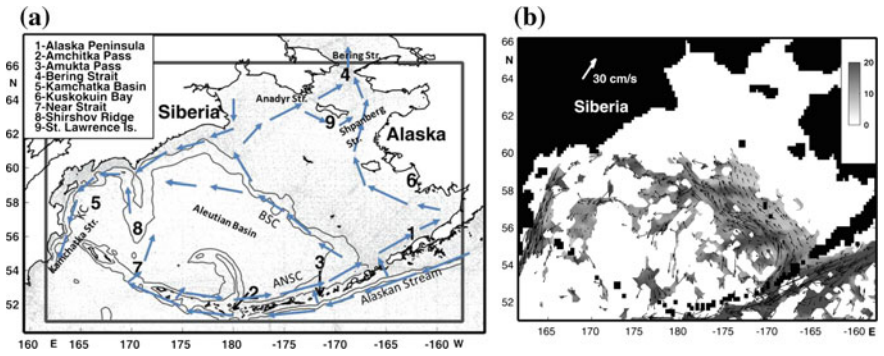

Fig. 1 **a** Spatial distribution of the historical temperature data in the Bering Sea. The model domain is shown by the rectangle. Contour lines mark the coastline and 1000 and 3000 m isobaths. Arrows show the schematic of the Bering Sea circulation according to Stabeno et al. [28] including the Bering Slope Current (BSC), the Aleutian North Slope Current (ANSC), and the Kamchatka Current (KC). **b** The multiyear mean surface drifter velocities averaged over the model grid cells. Gray shading shows the rms variance (cm/s) of the drifter velocity in each grid cell

Climatological Seasonal States of the Bering Sea

In oceanography, the volume of the in situ observations is usually insufficient to control all the model degrees of freedom, resulting in an ill-conditioned inverse problem. A reliable climatological evolution of the sea state is one of the best options for specifying the background state needed for regularization of the ill-conditioned inverse problem. Conventionally, the gridded climatological TS distributions are derived from historical observations using an optimal interpolation (OI) technique (e.g. [11]), which does not take into account the dynamical constraints and often leads to oversmoothing. On the contrary, the 4dVar DA obtains climatological states through the quasi-stationary variational DA approach [30]. Dynamical constraints of the model naturally introduce inhomogeneous advective smoothing in the regions of strong currents. This process allows for the derivation of a high resolution climatological state where all variables are dynamically balanced, which is not the case for "conventional" oceanographic Atlases derived through optimal interpolation algorithms.

This 4dVar approach was applied for the Bering Sea (BS) with a goal of obtaining the climatological annual mean and four seasonal states. The model was configured for the domain shown in Fig. 1a in a non-eddy-resolving mode on a relatively coarse (~18 km) regular z-coordinate grid with meridional and zonal resolutions of 0.16° and 0.3°, respectively, and a time step of 4 h. Vertically, the grid has 34 levels with unequal spacing ranging from 5 m near the surface to 500 m in the deeper layers. All data sets, outlined in section "The Regional 4dVar Data Assimilation System", were used to constrain the model solution. As a result, the annual mean climatological and four seasonal states were obtained. They are available at http://people.iarc.uaf.edu/~gleb/nprb_aleutian_passes/bering_sea_atlas_register.php.

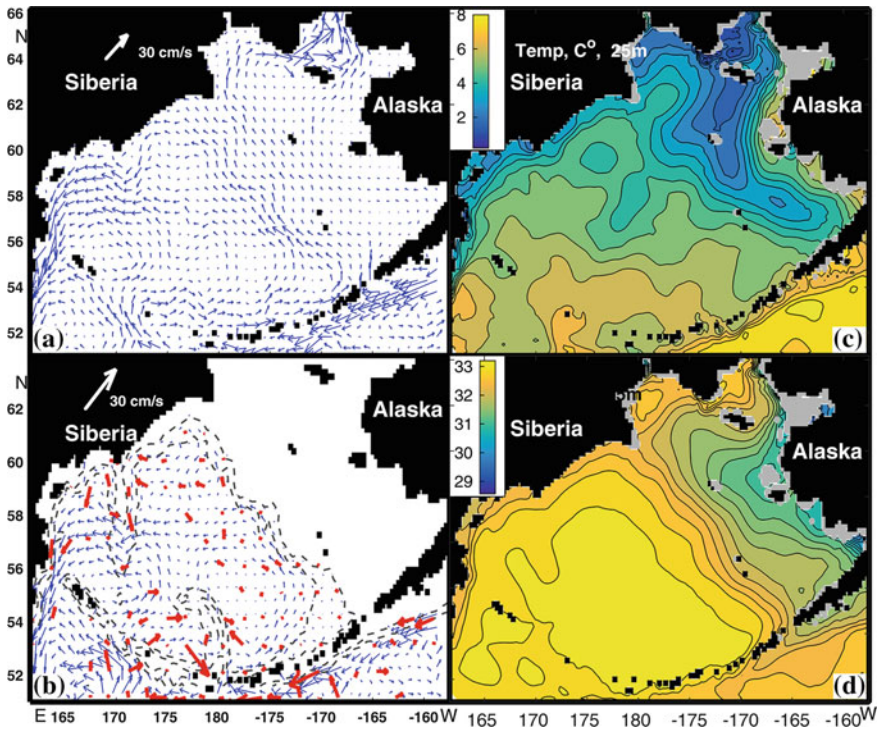

Fig. 2 Optimized maps of velocities at 25 m (**a**) and 1000 m (**b**) and temperature (**c**) and salinity (**d**) in summer. Red arrows denote mean velocities at 1000 m estimated from Argo floats parked at 1000 m [33]

Figure 2a–d presents the reconstructed mean summer state of the Bering Sea. The structure of the reconstructed circulation (Fig. 2a, b) is in good agreement with the schematic of the Bering Sea circulation provided by Stabeno et al. [28]. The circulation pattern reveals an intense (30–50 cm/s) Alaska Stream, a somewhat weaker (10–20 cm/s) Aleutian North Slope Current flowing along the southern and northern flanks of the Aleutian Arc and a cyclonic circulation in the deep part of the Bering Sea that includes a relatively weak (5–15 cm/s) Bering Slope Current and more pronounced (30–40 cm/s) Kamchatka Current along the eastern and western Bering Sea shelves, respectively. According to Fig. 2a, b, a significant portion of the inflow through the Near Strait forms a cyclonic gyre in the south-western part of the Bering Sea and then merges with the Kamchatka Current. The other portion of the Kamchatka Strait outflow comes from the Bering Slope Current that originates from multiple inflows through the eastern Aleutian Passes. The Alaskan Stream is the most intense current in the region. It flows along the southern flank of the Aleutian Arc and feeds the flows through the Aleutian Passes [29]. The Bering Slope Current splits into two branches near the point 57° N, 180° E. This is in a good qualitative agreement with the flow pattern described by Stabeno et al. [28],

but additionally, provides a statistically reliable quantification of the transport. The mean relative mismatch between the reconstructed surface velocities (Fig. 2a) and assimilated drifter velocities is 0.67.

Figure 2b provides a comparison of the optimized velocity field at 1000 m with independent (not assimilated) velocity data derived from the Argo floats. The average speed of the Argo floats is 4.6 cm/s, which is close to the mean optimized velocity amplitude of 3.7 cm/s. This 25% difference can be considered to be in reasonable agreement with the observations since a significant fraction of the ARGO drifters are involved in transient eddy motions resulting in higher Lagrangian mean velocities compared to the Eulerian mean speed estimates.

Figure 2c, d shows the summer TS distributions in the BS. In comparison with the optimal interpolation results (e.g., https://www.nodc.noaa.gov/OC5/PACIFIC2009/), the reconstructed fields are less smoothed, especially in the Northern Bering Sea (NBS) and along the Aleutian Arc. These are signatures of the strong topographically controlled flows through the Bering and Anadyr Straits and through the island system of the Aleutian Arc. The most important advantage of these TS distributions is that they are dynamically balanced with corresponding velocity fields (Fig. 2a, b), which allows for identifying finer structures of regional circulation while simultaneously providing estimates of climatological mass, heat and salt transports.

Except for the summer season, Pacific water masses entering the Bering Sea within the upper subsurface layer are characterized by higher temperature and salinity than the water mass residing in the Bering Sea at the same depth (Fig. 2c, d). The major cause of such temperature/salinity signal is due to the relatively high heat and salt content of the Pacific Water compared to the Bering Sea Water, as well as intense vertical and lateral mixing in the Aleutian Passes.

In the summer season, the warmest and least salty subsurface layer waters are formed in the nearshore regions of Bristol Bay, Norton Sound, and the Gulf of Karaginski. The presence of warm and relatively fresh salty waters in these areas is a consequence of strong stratification observed after the melting of the sea-ice cover and relatively weak winds, which are not able to mix the upper warm layer with the waters underneath. A somewhat colder and saltier upper subsurface layer water is present in the summer in several regions of the Bering Sea (e.g. in the central and eastern parts of the Aleutian Arc, and in the Chirikov Basin, Fig. 2c, d). Due to intense tidal and non-periodical currents in these regions, surface waters are mixed with the underlying cold waters formed in the winter and fall.

The optimized estimates of the mean volume transport through the major Aleutian Passes are found to be 2.5–7 times larger than those in the dynamical method [28]. This discrepancy is likely due to significant underestimation of the barotropic velocity component in the Aleutian Straits by the dynamical method. The latter suggestion is well supported by recent velocity observations in several Aleutian Passes, which reveal significant northward flow at a 100–200 m depth [29], indicating the importance of the regional barotropic flow in the overall Bering Sea volume balance.

Another important advantage of the 4dVar DA in the reconstructed climatological state of the Bering Sea is obtaining the dynamically balanced Sea Surface Height (SSH), which can formally be treated as MDOT, or the "*difference between a time-averaged SSH and geoid*". The importance of the MDOT availability is closely connected to the possibility of retrieving absolute SSH from the satellite altimetry anomalies observed by various satellite platforms (e.g. TOPEX/Poseidon, Jason-1/2, Earth Resources Satellite (ERS)-1/2, Envisat, Saral, etc.). Therefore, a number of research groups have developed methods to combine various data with altimetry to obtain more accurate estimates of the global MDOT [13, 18, 26]. For various reasons, all of these products have substantial deficiencies in the Bering Sea.

Figure 3 compares 4dVar MDOT and three other MDOT products in the region. Since the optimized surface velocities below the Ekman layer are in approximate geostrophic balance with the MDOT (optimized SSH field), the reconstructed MDOT contours (Fig. 3a) are conveniently interpreted as streamlines of the mean geostrophic currents at the surface. The circulation pattern reveals the following major structures: (a) an intense (30–40 cm/s) Alaskan Stream south of the Alaska Peninsula; (b) a somewhat weaker (10–20 cm/s) Aleutian North Slope Current embracing the southern and northern flanks of the Aleutian Arc; (c) the 30–40 cm/s

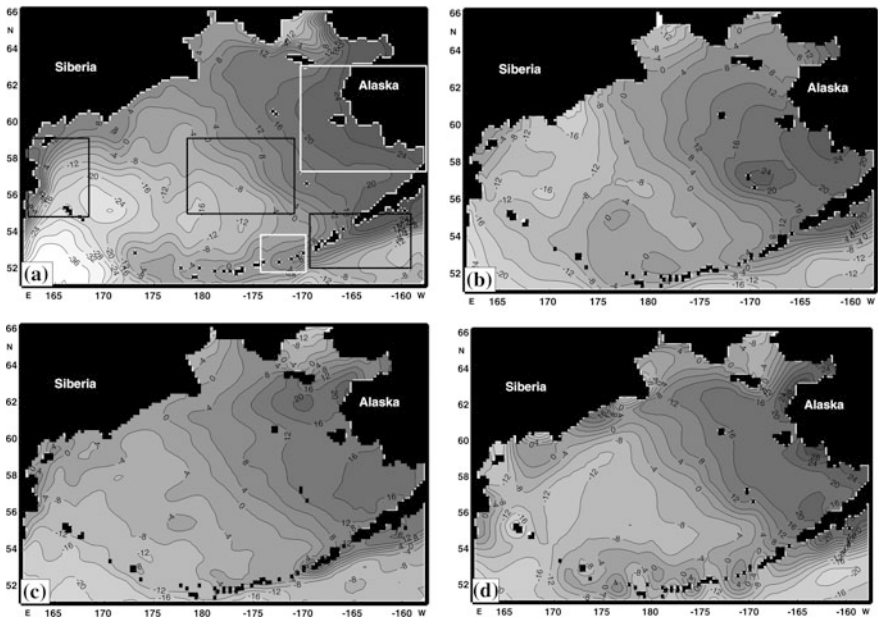

Fig. 3 The mean dynamic topographies of the Bering Sea **a** this study, **b** by Rio et al. [26], **c** by Rio et al. [27], and **d** by merging the EGM08 geoid model with altimeter data. Black rectangles in Fig. 3a show the drifter validation regions. White rectangles show the domain of high resolution SIOM DAS for the Amukta Pass and part of the Eastern Bering Sea shelf discussed below

strong Kamchatka Current to the west; and (d) a relatively weak (5–15 cm/s) cyclonic circulation occupying the deep part of the Bering Sea (Figs. 2a and 3a). According to Fig. 3a, a significant portion of this cyclonic gyre originates in the Near Strait with the rest coming from the inflow through other Aleutian passages. The circulation shown in Fig. 3a is in good qualitative agreement with the results of Stabeno et al. [29] who describes a gradual leakage of the Alaskan Stream though the passages in the Aleutian Arc.

The mean relative mismatch between the reconstructed surface velocities and assimilated drifter velocities (Fig. 1a) is 8.2 cm/s. It is unlikely that a better agreement could be obtained between the climatological velocity with mean amplitude of approximately 10 cm/s and the highly variable surface currents derived from the drifter trajectories affected by eddies and small-scale variations of the wind stress.

The derived MDOT were validated using the standard AVISO methodology: three regions well-covered by drifters were selected, gridded AVISO SSH anomalies from www.aviso.oceanobs.com were added to each MDOT, and the resulting geostrophic currents were compared with the currents deduced from drifter trajectories for the three regions shown by black rectangles in Fig. 3. The validation has shown that 4Dvar MDOT significantly (10–35%) outperforms all other MDOT products [22].

Obtaining a high resolution regional MDOT and its posterior errors is a prominent feature delivered by the 4dVar analysis of the climatological observations. In the next sections, we show how the derived MDOT benefits the analyses of decadal variability and hindcasts of the BS circulation at interannual time scales.

4dVar Analysis of the Circulation in the Aleutian Passes

This section provides another illustration that a realistic MDOT is a key component of a regional data assimilation system. In application to the regions with complicated topography, such as Aleutian Passes, MDOT inaccuracies may result in significant underestimation of the volume transports. To illustrate this, the 4dVar DA system was configured at a 6 km resolution with a domain around the Amukta Pass shown by the smaller white rectangle in Fig. 3a. A larger rectangle shows the domain of a similar experiment conducted in the central part of the Eastern Bering Sea shelf (see [23]).

Amukta Pass is one of the most important pathways for the inflow of the Pacific Water into the Bering Sea. Two assimilation experiments have been conducted in the domain: In the first experiment, the circulation for the period between January 10 and February 5, 2002 was reconstructed by assimilating AVISO sea level anomalies referenced to the 4dVar MDOT (Fig. 3a) in combination with the NCEP sea surface heat, salt and momentum fluxes. Climatological (winter) temperature/salinity in the Amukta Pass distributions were utilized as a first guess. The second

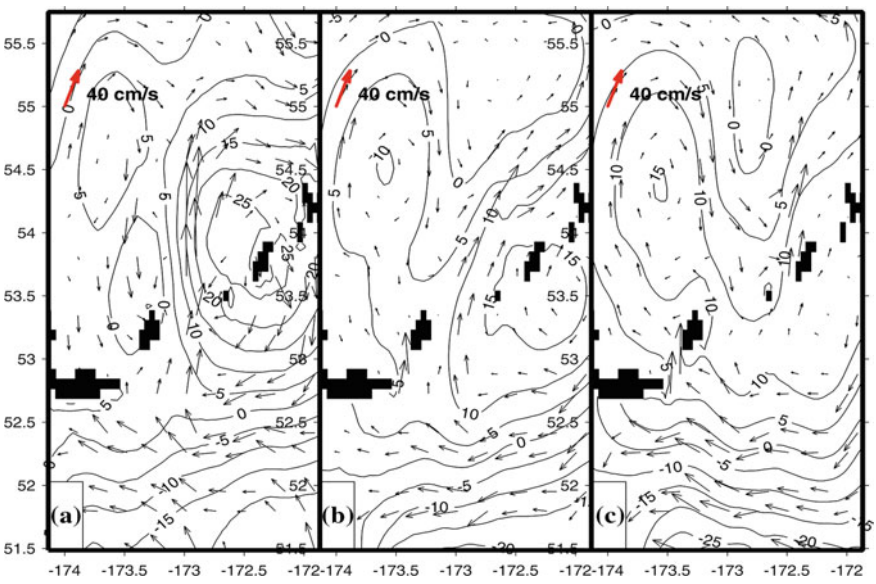

Fig. 4 Circulation in Amukta Pass on January 15 (**a**) and February 1 (**b**), 2002, derived by assimilation of the AVISO sea level anomaly data referenced to the MDOT shown in Fig. 3a. Panel (**c**) shows the circulation in the Amukta Pass on February 1, 2002, derived by assimilation of the AVISO sea level anomaly referenced to Fig. 3c (RIO05)

experiment had an identical configuration except that the 4Dvar MDOT was replaced by the RIO05 MDOT (Fig. 3c).

The mean circulation patterns on January 10–20 and January 25–February 5 derived in the first experiment are shown in Fig. 4a, b. The Amukta Pass northward transports in these two periods were 6.1 Sv and 3.5 Sv, respectively. A very intense northward current on January 10–20 and January 25-February 5 agrees well with the large positive anomalies of 7 Sv and 4 Sv in the Amukta transport observed by Stabeno et al. [29], who used records from four bottom-mounted ADCPs deployed in the region for 2 years [29]. Note that resolution of the gridded climatological MDOT (~18 km) and AVISO sea level anomaly (1/3° × 1/3°) are not sufficient enough to resolve the complicated geometry of the Amukta Pass. Therefore, better agreement with observation may be expected, if higher resolution climatological MDOT and/or AVISO products were available.

On the contrary, Fig. 4c demonstrates a much weaker circulation around the Amukta Pass which was derived by assimilating AVISO sea level anomalies referenced to the RIO05 MDOT shown in Fig. 3c. The respective transport averaged over the period of January 25-February 5, 2002 is close to 1.6 Sv, which is 2.5 times smaller than 4 Sv observed by Stabeno et al. [29]. These experiments indicate that RIO05 significantly underestimates the MDOT gradient in the region of the

Aleutian Passes. In the context of the Bering Sea large-scale dynamics, accurate MDOT appears to be especially important since the processes of the ventilation of the deep and shallow parts of the BS occurs through the few relatively narrow Aleutian Passes. These ventilation processes are one of the key mechanisms controlling the BS ecosystem and, therefore, should be reconstructed with increased accuracy.

In relation to ecosystem dynamics, the vast shelf of the Eastern Bering Sea (EBS) represents the major hub located on the crossroads of the pathways between the Pacific and Arctic Oceans. Extreme complexity of the advective and mixing processes in the shallow waters of EBS shape the seasonal ecosystem parameters and require accurate treatment in terms of observational and dynamical consistency.

Eastern Bering Sea: Regional Ocean in Motion

The Eastern Bering Sea (EBS) plays an important role in United States' fisheries, dynamics of the immense populations of marine birds and mammals, and subsistence activities of native communities. Therefore, this region has been permanently studied in the last decades. The most comprehensive studies were conducted in 2007–2010 in the framework of the Bering Sea Integrated Ecosystem Research Program (BSIERP). Typically, 2–3 hydrophysical (CTD) surveys per year were conducted and 3 mooring arrays were supported during 2007–2010 (Fig. 5). Note, however, that each CTD survey usually lasts for 2–3 weeks, providing only a "snapshot" of a limited area of the EBS, while during the rest of the year, there is no reliable information about the hydrophysical state. At the same time, moorings provide continuous time series in a few locations lacking adequate spatial coverage. Obviously, these data cannot adequately describe the circulation in the entire EBS, if considered, without additional dynamical constraints. The 4dVar DA provides a good guide on how to combine observations from different sources for reconstructing the non-stationary state of the ocean in motion.

Nested 4dVar system. The BSIERP observations and other sources of data provide an excellent opportunity to improve our understanding of changes in the physical forcing of the Bering ecosystem in its response to the climate change. But due to ice coverage in the winter, a relatively large regions of the EBS including the key passages through the Anadyr and Bering Straits were not covered by these studies. In view of the necessity to adequately resolve the Bering and Anadyr Straits, a nested SIOM 4dVar DA system was developed. The nested DA system utilized as a first guess, the momentum, heat and salt fluxes from Bering Ecosystem Study Ice Ocean Modeling and Assimilation System (BESTMAS) [10, 36].

The nested models were configured in the domains shown in Fig. 5 with a resolution of 7 km for the fine model grid, ω, embedded into a coarser (15–20 km) grid, Ω (Fig. 1). In the vertical, the coarse (fine) resolution model had 35(15) unevenly spaced levels with 5 (2.5) m near-surface spacing, which increased to 500(25) m at

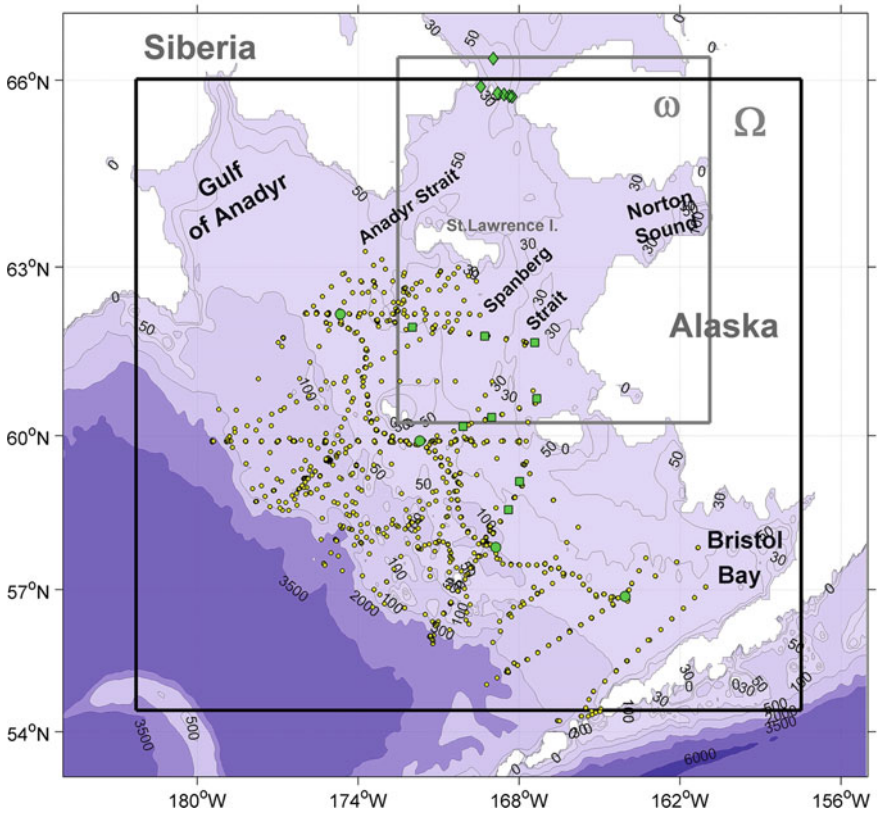

Fig. 5 Model domain and assimilated observations. The boundaries of the coarse (17 km) and fine (7 km) resolution grids are shown by the black and gray rectangles, respectively. Small circles show hydrographic stations, and mooring locations from different observational experiments are shown as white circles, squares, and diamonds

the bottom. Trajectories of both models were controlled by the initial/boundary conditions and surface fluxes. The details and validation of the novel two-way nested DA iterative algorithm were discussed in Panteleev et al. [25]. It was shown that the nested DA approach allows for a much better reconstruction of the flow through the Bering Strait and a significant reduction of the model-data observation misfits in comparison with the BESTMAS data assimilative solution. In the entire range of the velocity observations from moorings, 4dVar velocities demonstrate a much better linear fit to the data compared to the one characterizing the BESTMAS solution [25].

The two-way nested 4dVar scheme allowed us to achieve much better consistency between the optimal solutions within the nested domains. As a result, a significantly better fit was obtained to SSH data, constraining circulation in a coarse resolution domain, and to higher resolution velocity data controlling the Bering Strait throughflow.

The major sources of data needed for model forcing and assimilation are shown in Fig. 5 and include velocity observations from three mooring arrays; multiple CTD surveys. In addition, we assimilate the gridded SSH anomalies from the AVISO data set referenced to the regional MDOT and background information from the reconstructed seasonal climatologies of the Bering Sea (Section "The Regional 4dVar Data Assimilation System").

The optimized evolution of the EBS state was obtained by assimilating the above described data over 49 4-week time windows spanning the period of January 1, 2007 to October 3, 2010. On the average, $300 \times 4 = 1200$ iterations were required to achieve the nested 4dVar convergence of a single 4-week problem.

Mass, heat and freshwater transports. The 4dVar-optimized weekly averaged fluxes are shown in Fig. 6 in the Bering and Anadyr Straits. Because mass is conserved, and the surface heat/freshwater fluxes in the Northern Bering Sea can be neglected, the difference between the curves gives an insight on the partitioning of the respective Bering Strait transports between the Anadyr and Spanberg inflows. The heat and freshwater transports in Fig. 10 were obtained relative to −1.9 °C and 34.8 psu, respectively.

An interesting feature in Fig. 6 are the events when the Bering Strait fluxes were much larger than the advective heat/freshwater transports entering the Chirikov Basin through the Anadyr Strait (e.g., September, November 2007, August–September 2010). Near-surface circulation and wind stress patterns (Fig. 7a, c)

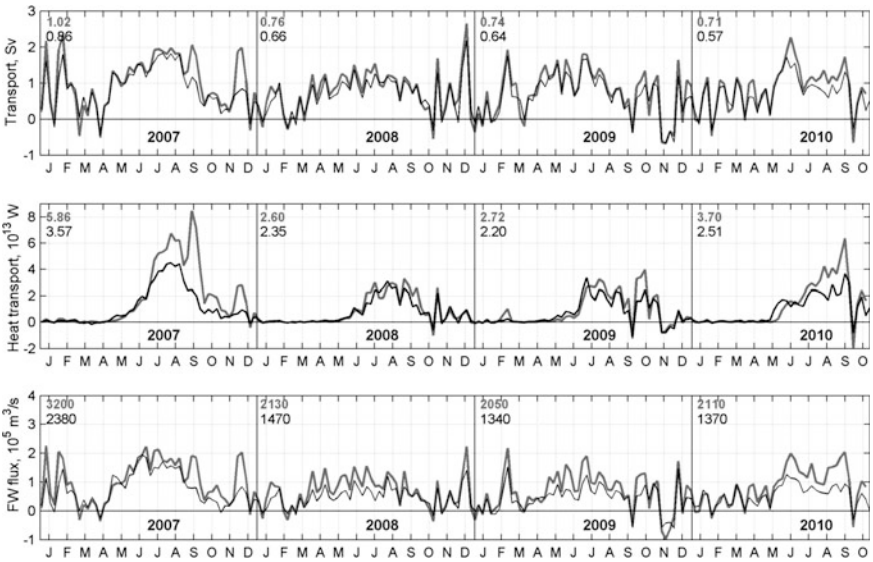

Fig. 6 Evolution of the weekly averaged mass, heat, and freshwater fluxes through the Bering (thick gray line) and Anadyr Straits (solid black line). Annual mean values of the fluxes are shown in the upper right corners of the respective boxes. The units are, respectively, 10^6 m^3/s, 10^{20} J, and 10^3 m^3/s

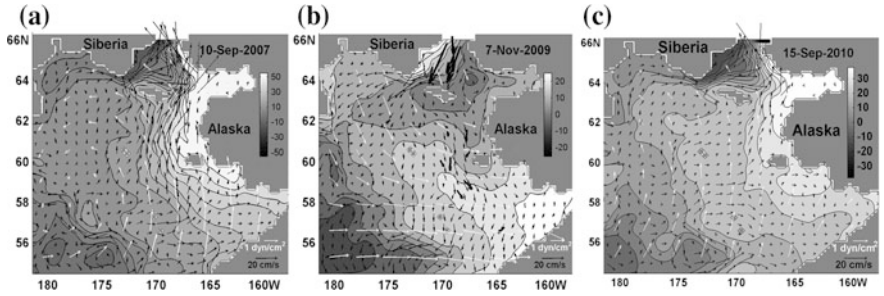

Fig. 7 Velocity at 25 m depth (black arrows), wind stress (white arrows), and SSH (shading, cm), at 0.00 UTC on September 10, 2007, November 7, 2009, and September 2, 2010. Thick arrows in the middle of the plot show velocities observed on the moorings

indicate that these anomalies were caused by strong southeasterly winds over the EBS shelf, which raise the sea level along the Alaskan coast and enhance transport of the warm and fresh waters through the Spanberg Strait.

Wind stress patterns in Fig. 7a, c indicate that intensification of the northward current along the Alaskan coast was forced by atmospheric lows over the central Bering Sea. Such cyclones are quite a common phenomena in late fall/winter and are known to cause intensification of the Kamchatka Current [7]. However, since EBS is mostly ice covered in winter, these winds have little effect on the heat transport, but may cause a noticeable increase in the freshwater transport (lower panels in Fig. 6). In summer, strong southeasterly winds associated with cyclones over the BS basin are less common, although a certain increase in the summer storm activity has been documented [14] over the last decade. These storms may contribute significantly to the observed decrease of the ice cover in the Chukchi Sea. Winter storms have a larger impact on the deep mixing in the central BS and freshwater flux through the Bering Strait.

Another interesting phenomena in Fig. 6 are the anomalous (southward) transport events through the Bering Strait. Most of them occur in fall-winter and have a typical duration of 1–2 weeks. The exception is a 28-day southward transport observed in November 2009. Comparison with the wind forcing has shown that all the negative transport anomalies in September–November 2008–2010 are associated with the southward winds. This phenomenon has been documented by Coachman [4] and appears to be a typical feature for the freezing and (to a lesser extent) melting seasons. It is also remarkable that in 2007–2010, the reversing of the Bering Strait throughflow mostly occurred synchronously with the Anadyr Current, when the contribution of the Spanberg Strait volume transport becomes negligible. Analysis of the optimized circulation shows that forcing by the northeasterly winds completely blocks the Spanberg Strait throughflow causing dramatic structural changes in the SSH and circulation patterns. Northwesterly wind surge tends to change the sign of the large-scale SSH gradient in the southern EBS (cf. Fig. 7a–c) and completely reverse the flow field in the Bering Strait along the Alaskan and Siberian coastlines. Prolonged flow reversals, such as the one observed

in November 2009, may have a significant impact on the EBS ecosystem by affecting the residence times and displacing the cold pool (e.g. [3]) boundary which is advected by the general southward flow clearly seen in Fig. 7b on a larger scale.

Water pathways and residence times. Analysis of trajectories of the Lagrangian particles is a convenient approach to study the regional ecosystems (e.g. [2, 19]). It could be also useful in the analysis of water mass pathways and their transformation rates (e.g. [22]). In the analysis described below, we focus on two important sub-regions: the Unimak Strait (the easternmost passage from the open Pacific into the EBS) and the BSC source region properly located north of Unalaska Island. Lagrangian particles were released in each region once a week during 3.5 years. Trajectories of the fastest and slowest particles from these releases are shown in Fig. 8a. It is noteworthy that the largest residence times τ (up to 40 months) were observed exclusively for the particles released in the Unimak Pass while the smallest residence times (8–10 months) were documented for the particles released north of Unalaska Island, where the North Alaskan Slope Current meets the EBS continental slope. The residence time distributions in both regions (Fig. 8b) are quite different in shape. The Unalaska release region is characterized by a double peak structure. A more detailed analysis shows that the fastest particles, corresponding to the first peak at $\tau = 10$ months were mostly released in the fall season (October-November), when the BSC is spun up by the storm activity [24]. The majority of Unalaska released particles reach the Arctic Ocean in 11–15 months as they travel with the BSC of normal strength. The near-exponential tail of the distribution ($\tau \sim$ 16–35 months) is formed by the particles carried by mesoscale eddies across the continental slope into the EBS shelf.

In contrast to the Unalaska particles, particles released at Unimak Pass are characterized by much more homogeneous distribution over the residence times (thin line in Fig. 8b). This could be explained by the low probability of their capture by the core of the BSC. As a consequence, most of these particles start their travel

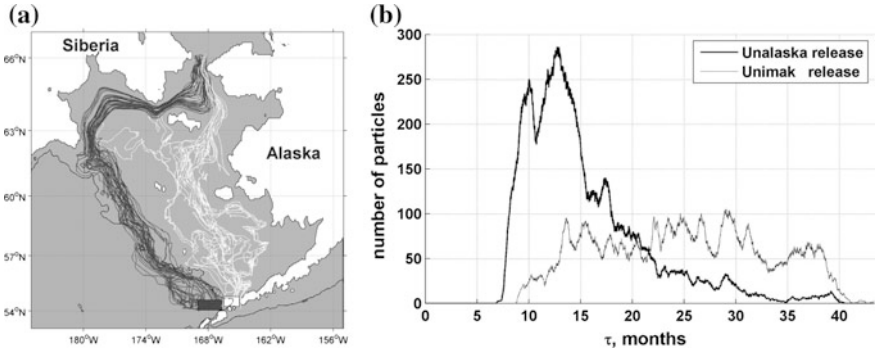

Fig. 8 **a** Trajectories of the particles reaching the Bering Strait and released in the Unimak Pass (white rectangle) and north of the Unalaska Island (dark gray). **b** EBS residence time distribution of the particles released in the Unimak Pass (thin line) and north of Unalaska Island

history in the EBS shelf environment which is characterized by much weaker and less organized currents. Trajectories of the Unimak Pass particles with the largest residence times ($\tau \sim 35$–40 months) shown in Fig. 8b first wander around the southern EBS shelf west of the Pribilof Islands, and then slowly proceed north following the Spanberg Strait pathway to the Arctic Ocean. Only a small fraction of these particles join the Anadyr Current far downstream, and they are never engaged in the eddy-induced exchange with the BSC. The same property characterizes the fastest particles populating the left peak ($\tau < 11$ months) of the Unalaska distribution in Fig. 8b. These particles strictly follow the main stream of the BSC and Anadyr Current.

Summary

We presented a systematic approach for developing a regional DAS as applied to the Bering Sea. The method is based on applying the 4dVar technique to both climatological and instantaneous data with the ultimate goal of reconstructing dynamically and statistically consistent states at various temporal and spatial scales: from large-scale interannual circulation to eddy resolving transient current systems. The backbone of the system are dynamically balanced seasonal climatological states and the corresponding MDOT of the Bering Sea, which distinguishes the developed Bering Sea DAS from other regional systems developed in the last decade, such as for the Oregon Coast by Kurapov et al. [8], and for the Hawaiian Islands by Janekovich et al. [6].

The developed seasonal climatologies of the Bering Sea include dynamically consistent temperature, salinity, velocity, and sea surface height fields for each season (winter, fall, spring and summer) and the corresponding fields for the climatological mean state of the Bering Sea. These climatologies have sufficiently fine resolution to allow accurate specification of the dynamically balanced background state for any subregion of the Bering Sea. An important by-product is the high-resolution regional MDOT, whose accuracy and quality significantly outperforms the other MDOTs derived from various global reanalyses.

Combining the developed Bering Sea MDOT with instantaneous satellite altimetry data provided an important observational constraint on the regional dynamics in the entire Bering Sea. The 4dVar assimilation of satellite altimetry anomalies referenced to the 4Dvar MDOT provides much better estimates of the transport through the Aleutian Passes. These flows control the supply of nutrients to the Bering Sea, affect the stability of the Aleutian North Slope Current and the process of eddy formation along the Aleutian Arc, which is an important component of local ecosystem dynamics.

The seasonal climatologies were also used to constrain a more detailed and comprehensive study of the EBS circulation in 2007–2010 by means of the nested 4dVar DAS developed by Panteleev et al. [25]. Comparison with the BESTMASS DA system of Lindsay and Zhang [10] has shown that the new DAS

provides a more realistic EBS circulation and Bering Strait throughflow both in terms of model-data misfits and general dynamical consistency. This allows for a more accurate analysis of the property exchange processes between the Pacific Ocean and the Bering Sea, including residence times, pathways and the transformation rates of various water masses on their way to the Arctic Ocean.

The wealth of new information on the Bering Sea dynamics delivered by the developed DAS illustrates the importance of regional DA systems for further improvement in understanding and forecasting environmental conditions in the marginal seas and nearshore areas. Our experience shows that 4dVar reconstruction of the dynamically consistent regional climatologies is of particular importance for the reanalysis of the local data sets. In turn, the improved accuracy of the hindcasts would inevitably result in better forecasting of the regional environmental conditions that are extremely important in many applications.

Acknowledgements This study was supported by the University of Hawaii, the International Arctic Research Center, NSF grants 1107925, 1203740 and ARC-1107327. G. Panteleev and M. Yaremchuk were also supported by the ONR core project "Arctic data assimilation" and program element 0602435N as part of the project "Adjoint-free 4dVar for Navy ocean models". The authors are indebted to P. Stabeno for providing drifter and current data.

References

1. Brasseur, P. (1991). A variational method for the reconstruction of general circulation fields in the Northern Bering Sea. *Journal Geophysical Research, 96,* 4891–4907.
2. Carlotti, F., & Wolf, K.-U. (1998). A Lagrangian ensemble model of Calanus finmarchicus coupled with a 1-D ecosystem model. *Fisheries Oceanography, 7*(3/4), 191–204.
3. Cianelli, L., & Bailey, K. M. (2005). Landscape dynamics and resulting species interactions: The cod-capelin system in the southeastern Bering sea. *Marine Ecology Progress Series, 291,* 227–236.
4. Coachman, A. K. (1993). On the flow field in the Chirikov Basin. *Continental Shelf Research, 13,* 481–492.
5. Forget, G., Campin, J.-M., Heimbach, P., Hill, C. N., Ponte, R. M., & Wunsch, C. (2015). ECCO version 4: An integrated framework for non-linear inverse modeling and global ocean state estimation. *Geoscientific Model Development Discussions, 8,* 3653–3743. https://doi.org/10.5194/gmdd-8-3653-2015.
6. Janekovich, I., Powell, B. S., Matthews, D., McManus, M. A., & Sevadjian, J. (2013). 4D-Var data assimilation in a nested, coastal ocean model: A Hawaiian case study. *Journal Geophysical Research, 118,* 1–14.
7. Hughes, F. W., Coachman, L. K., 7 Aagard, K. (1974). Circulation transport and water exchange in the western Bering Sea. In D. W. Hood and E. J. Kelly (Eds.), *Oceanography of the Bering Sea with emphasis on the renewable resources* (pp. 59–98). Institute of Marine Science, University of Alaska, Fairbanks.
8. Kurapov, A. L., Foley, D., Strub, P. T., Egbert, G. D., & Allen, J. S. (2011). Variational assimilation of satellite observations in a coastal ocean model off Oregon. *Journal Geophysical Research, 116,* C05006. https://doi.org/10.1029/2010JC006909.
9. Le Dimet, F. X., & Talagrand, O. (1986). Variational algorithms for analysis and assimilation of meteorological observations: Theoretical aspects. *Tellus Series A, 38,* 97–100.

10. Lindsay, R. W., & Zhang, J. (2006). Assimilation of ice concentration in an ice-ocean model. *Journal of Atmospheric and Oceanic Technology, 23,* 742–749.
11. Luchin, V., Kruts, A., Sokolov, O., Rostov, V., Rudykh, N., Perunova, T., et al. (2009) Climatic Atlas of the North Pacific Seas 2009: Bering Sea, Sea of Okhotsk, and Sea of Japan. In V. Akulichev, Yu. Volkov, V. Sapozhnikov and S Levitus (Eds.), *NOAA Atlas NESDIS 67* (380 pp.). U.S. Government Printing Office, Washington, D.C., CD Disc.
12. Madec, G., Delecluse, P., Imbard, M., et al. (1999) OPA 8.1 Ocean General Circulation Model. Reference Manual, Note du Pole de Modelisation (Institut Pierre-Simon Laplace (IPSL), France.
13. Maximenko, N., Niiler, P., Rio, M.-H., Melnichenko, O., Centurioni, L., Chambers, D., et al. (2009). Mean dynamic topography of the ocean derived from satellite and drifting buoy data by three different techniques. *Journal of Atmospheric and Oceanic Technology, 26*(9), 1910–1919.
14. Mesquita, M. S., Atkinson, D. E., & Hodges, K. I. (2010). Characteristics and variability of the storm tracks in the North Pacific, Bering Sea and Alaska. *Journal of Climate, 23,* 294–311. https://doi.org/10.1175/2009/JCLI3019.1.
15. Moore, A. M., Arango, H. G., Broquet, G., Edwards, C., Veneziani, M., Powell, B., et al. (2011). The regional ocean modeling system (ROMS) 4-dimensional variational data assimilation systems Part II. Performance and application to the california current system. *Progress in Oceanography, 91*(1), 50–73.
16. Nechaev, D. A., & Yaremchuk, M. I. (1994). Conductivity-temperature-depth data assimilation into a three-dimensional quasigeostrophic open ocean model. *Dynamics of Atmospheres and Oceans, 21,* 137–165.
17. Nechaev, D., Panteleev, G., & Yaremchuk, M. (2005). Reconstruction of the circulation in the limited region with open boundaries: Circulation in the Tsushima Strait. *Okeanologiya, 45*(6), 805–828.
18. Niiler, P., Maximenko, N., & McWilliams, J. (2003). Dynamically balanced absolute sea level of the global ocean from near-surface velocity observations. *Geophysical Research Letters, 30* (22), 2164. https://doi.org/10.1029/2003/GL018628.
19. Panteleev, G. G., deYoung, B., Reiss, C., & Taggart, C. (2004). Passive tracer reconstruction as a least squares problem with a semi-lagrangian constraint: An application to fish eggs and larvae. *Journal of Marine Research, 62,* 787–878.
20. Panteleev, G., Nechaev, D., & Ikeda, M. (2006). Reconstruction of summer Barents Sea circulation from climatological data. *Atmosphere-Ocean, 44*(2), 111–132.
21. Panteleev, G. G., Proshutinsky, A., Kulakov, M., Nechaev, D. A., & Maslowski, W. (2007). Investigation of summer Kara Sea circulation employing a variational data assimilation technique. *Journal of Geophysical Research*, *112*, C04S15. https://doi.org/10.1029/2006jc003728.
22. Panteleev, G., Proshutinsky, A., Nechaev, D., Woodgate, R., & Zhang, J. (2010). Reconstruction and analysis of the Chukchi Sea circulation in 1990–1991. *Journal of Geophysical Research, 115,* C08023. https://doi.org/10.1029/2009JC005453.
23. Panteleev, G., Yaremchuk, M., Stabeno, P., Luchin, V., Nechaev, D., & Kukuchi, T. (2011). Dynamic topography of the Bering Sea. *Journal Geophysical Research, 116,* C05017. https://doi.org/10.1029/2010JC006354.
24. Panteleev, G., Yaremchuk, M., Nechaev, D., & Kikuchi, T. (2012). Variability of the Bering Sea circulation in 1992–2010. *Journal of Oceanography, 68,* 485–496. https://doi.org/10.1007/s10872-012-0113-0.
25. Panteleev, G., Yaremchuk, M., Francis, O., Stabeno, P. J., Weingartner, T., & Zjang, J. (2016). An inverse modeling study of circulation in the Eastern Bering Sea during 2007–2010. *Journal of Geophysical Research*, *121*, 3970–3989. https://doi.org/10.1002/2015jc011287.
26. Rio, M.-H., Schaeffer, P., Lemoine, J.-M., & Hernandez, F. (2005). Estimation of the ocean mean dynamic topography through the combination of altimetric data, in-situ measurements

and GRACE geoid: From global to regional studies. In *Proceedings of the GOCINA International Workshop*.
27. Rio, M.-H., Schaeffer, P., Moreaux, G., Bourgogne, S., Lemoine, J.-M., & Bronner, E. (2009). A new mean dynamic topography computed over the global ocean from GRACE data altimetry and in-situ measurements. In *Proceedings of OceanObs'09 Conference*, Venice, Italy.
28. Stabeno, P. J., Schumacher, J. D., & Ohtani, K. (1999). The physical oceanography of the Bering Sea. In *Dynamic of the Bering Sea* (838 pp.). Fairbanks: Alaska Sea Grant College Program.
29. Stabeno, P. J., Kachel, D. G., & Sullivan, M. E. (2005). Observation from moorings in the Aleutian Passes: Temperature, salinity and transport. *Fisheries Oceanography, 14,* 39–54.
30. Tziperman, E., & Thacker, W. C. (1989). An optimal-control/adjoint equation approach to studying the oceanic general circulation. *Journal of Physical Oceanography, 19,* 1471–1485.
31. Woodgate, R. A., Aagaard, K., & Weingartner, T. (2005). Monthly temperature, salinity, and transport variability of the Bering Strait through flow. *Geophysical Research Letters, 32,* L04601. https://doi.org/10.1029/2004GL021880.
32. Wunsch, C. (1996). *The ocean circulation inverse problem* (p. 442). Cambridge: Cambridge University Press.
33. Yoshinari, H., Maximenko, N. A., & Hacker, P. W. (2006). YoMaHa'05: Velocity data assessed from trajectories of Argo floats at parking level and at the sea surface. IPRC Technical Note No. 4, 20 pp.
34. Yaremchuk, M., & Sentchev, A. (2012). Multi-scale correlation functions associated with polynomials of the diffusion operator. *Quarterly Journal of the Royal Meteorological Society, 138,* 1948–1953.
35. Yaremchuk, M., Carrier, M., Smith, S., & Jacobs, G. (2013). Background error correlation modeling with diffusion operators, In S. K. Park and L. Xu (Eds.), *Data assimilation for atmospheric, oceanic and hydrologic applications* (Vol. II, pp. 177–203). Berlin, Heidelberg: Springer. https://doi.org/10.1007/978-3-642-35088-78.
36. Zhang, J., & Rothrock, D. A. (2005). The effect of sea ice rheology in numerical investigations of climate. *Journal Geophysical Research, 110,* C08014. https://doi.org/10.1029/2004JC002599.